Lab on a Chip

PAPER

View Article Online
View Journal

A 1024-sample serum analyzer chip for cancer diagnostics†

Cite this: DOI: 10.1039/c3lc51153g

Jose L. Garcia-Cordero‡ and Sebastian J. Maerkl*

We present a platform that combines microarrays and microfluidic techniques to measure four protein biomarkers in 1024 serum samples for a total of 4096 assays per device. Detection is based on a surface fluorescence sandwich immunoassay with a limit of detection of ~1 pM for most of the proteins measured: PSA, TNF-α, IL-1β, and IL-6. To validate the utility of our platform, we measured these four biomarkers in 20 clinical human serum samples, 10 from prostate cancer patients and 10 female and male controls. We compared the results of our platform to a conventional ELISA and found a good correlation between them. However, compared to a classical ELISA, our device reduces the total cost of reagents by 4 orders of magnitude while increasing throughput by 2 orders of magnitude. Overall, we demonstrate an integrated approach to perform low-cost and rapid quantification of protein biomarkers from over one thousand serum samples. This new high-throughput technology will have a significant impact on disease diagnosis and management.

Received 9th October 2013,
Accepted 25th November 2013

DOI: 10.1039/c3lc51153g

www.rsc.org/loc

Introduction

The primary applications of microfluidics in the health-care sector have been in the form of point-of-care (POC) medical diagnostic devices,[1] aimed at measuring one or a few analytes from a single sample, with reasonably fast turn-around times. While significant progress has been demonstrated it is still difficult to assess whether these technologies and their commercialization would outweigh the many advantages provided by centralized laboratories such as quality, cost reduction, assay sensitivity, specificity, reproducibility, regulations, and performance.[2] Disappointingly, little progress has been made in developing microfluidic devices capable of outperforming automated clinical sample analyzers in terms of throughput and cost reduction. Automated clinical sample analyzers are large, expensive robotic workstations capable of performing hundreds of tests per hour and are commonly found in centralized laboratories or hospitals. For example, the Cobas 8000 (e 602 module) from Roche and the Architect i4000SR from Abbot, amongst others, can perform up to 170 and 400 immunoassays per hour, respectively. This translates to 1530–3600 assays for a 9 h workday and 4080–9600 assays in 24 hours.

The importance of high-throughput immunoassays will continue to increase as more biomarkers are being identified and personalized medicine becomes prevalent. To monitor disease progression or predict disease risk will require analysis of a multitude of biomarkers including genomic, proteomic, transcriptomic, metabolomic, and autoantibody profiles.[3] However, current clinical sample analyzers do neither meet the demand in throughput nor drastically reduce the cost per assay, as the assay volumes are not significantly reduced when compared to standard bench-top ELISA assays. Thus, although a throughput of 9600 assays in 24 hours is reasonably impressive, microfluidic technologies could not only further enhance throughput, but also decrease the cost per assay dramatically, making large panel biomarker screening affordable and realistic. Any low-cost immunoassay technology for the large-scale analysis of samples would have a significant impact in clinical research, the diagnosis of diseases, and the monitoring of an individual's health, because tests could be performed more frequently without incurring additional costs on the health care system.

One approach to decrease the cost of immunoassays is to reduce the volume of reagents needed to run them (in particular the total volume of antibodies), which in turn requires reducing the sample volume. Reducing the amount of sample also has other implications because more analytes could be measured from the same sample, even for analytes for which an antibody has not yet been developed. This is particularly useful for samples stored in biobanks[4] or accrued during clinical studies. However, reducing sample volume alone is not sufficient, as it has to be accompanied by an integrated and automated approach to handle thousands of samples simultaneously so that costs can be further decreased while

Institute of Bioengineering, School of Engineering, École Polytechnique Fédérale de Lausanne (EPFL), Lausanne, Switzerland. E-mail: Sebastian.maerkl@epfl.ch

† Electronic supplementary information (ESI) available. See DOI: 10.1039/c3lc51153g

‡ Current address: CINVESTAV-Monterrey, PIIT, Nuevo León 66600, Mexico.

retaining the same assay quality and reproducibility. This approach is difficult to implement on very small volume scales using liquid handling robots.[5] Microfluidics is a more suitable alternative. While there have been a few attempts to measure analytes from nanoliter volume samples, they are limited in sample throughput and do not multiplex analytes.[6]

In this paper, we describe a microfluidic platform (Fig. 1), which combines microarraying and microfluidic techniques, to create an integrated microfluidic device capable of analyzing 4 biomarkers in 1024 nanoliter-volume samples for a total of 4096 assays per device. The platform increases the throughput of a previous device which we applied to a cell culture analysis by ~2.6 fold,[7] and we show here that the approach can be applied to quantitate biomarkers in clinical human serum samples. Compared to our previous platform, we redesigned the layout of the chip to fit 1024 assay units on the area of a microscope glass slide (75 mm × 25 mm), including the space required for 23 pressure control lines, 9 inlets, and 2 outlets.

Although operating at extremely low sample volumes of 5 nL, we were able to achieve similar sensitivities as a conventional ELISA, the current gold standard for protein biomarker quantitation. This unprecedented throughput, low sample volume consumption, and straightforward microfluidic design allow several improvements over ELISA: (i) the total volume and cost of reagents is decreased >40 000-fold, (ii) the amount of antibody is reduced >10 000, and (iii) the time to run an assay is reduced by ~20-fold.

Materials and methods

Device fabrication

Microfluidic devices were fabricated by multilayer soft-lithography, as previously described.[7] The control layer mold consisted of ~30 μm structures patterned on negative photoresist (GM1070, Gersteltec, Switzerland) whereas the flow layer mold was made with positive photoresist (AZ9260, Clariant GmbH, Germany) coated to a height of ~10 μm. The flow layer mold was baked at 180 °C in a convection oven for 1 hour to round the structures. Devices were cast in polydimethylsiloxane (PDMS, Sylgard 184, Corning, USA). PDMS was poured into the control mold to a thickness of 5 mm and was spin-coated on the flow layer mold at 2100 rpm for 60 s. Both molds were baked for 30 min at 80 °C. Chips from the control layer mold were cut, peeled from the mold, aligned to the flow layer mold, and baked for an additional 90 min at 80 °C. Aligned devices were again cut and peeled from the mold. Holes were punched using a precision manual-punching machine (Syneo, USA).

Surface chemistry and reagents

Microscope glass slides were coated with epoxysilane to covalently immobilize proteins to the surface of the glass.[8] Briefly, glass slides are bathed for 30 min in a mixture of 720 mL milli-Q water and ammonia solution (5 : 1 ratio) and 150 mL of hydrogen peroxide. Next, glass slides were incubated for 20 min in a solution of 1% 3-glycidoxypropyltrimethoxymethylsilane in toluene. The glass slides were dried and baked for 30 min at 120 °C in a convection oven, after which they were sonicated in toluene, rinsed with isopropanol, and blow-dried. Glass-slides were stored at room temperature in a vacuum-desiccator. Biotinylated bovine serum albumin, BSA (29130), neutravidin (31000), and 1% blocker casein in PBS (37528) were purchased from Thermo Fisher Scientific. Neutravidin conjugated with different fluorescent dyes (Dylight 488, 550, 650, Thermo Scientific) enhanced green fluorescent protein (E-GFP, 4999-100, BioVision), and biotinylated anti-GFP antibody (ab6658, Abcam) were also acquired.

Antibodies and proteins

Anti-human PSA monoclonal antibodies matched pairs (10-P20E and 10-P20D) and purified native human PSA protein (30C-CP1017U) were purchased from Fitzgerald Industries International (MA, USA). The rest of the anti-human antibodies matched pairs and human protein standards were bought from eBioscience: IL-6 biotin-conjugate (13-7068-81),

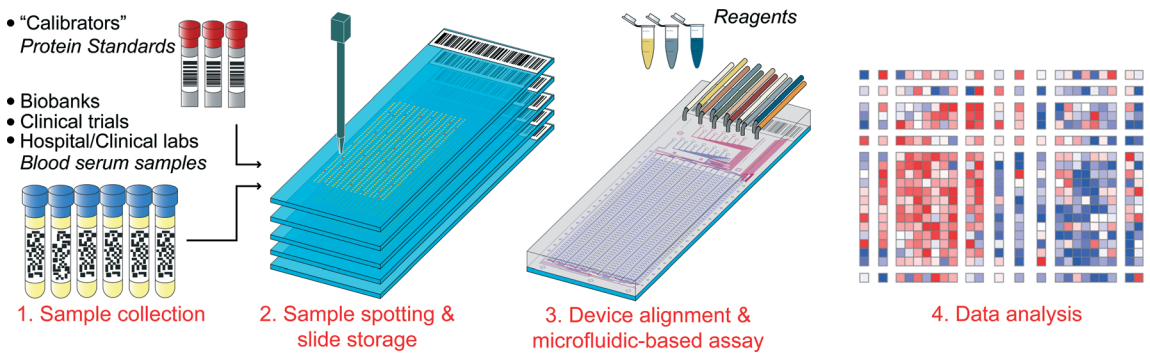

Fig. 1 Workflow for massively parallel immunoassays of clinical samples. Samples collected from biobanks, clinical trials, hospitals, or clinical laboratories are automatically spotted with a microarray robot. Protein standards are also spotted on the same array to serve as an internal calibration standard. A microfluidic device is aligned to the array. Eight different reagents are needed to operate the chip. Tubing is connected to the chip to control fluid movement. The chip is run the next day with minimum operator intervention. Data are analyzed and reported to the clinician or researcher.

IL-6 PE-conjugate (12-7069-81), IL-6 protein standard (39-8069-65), IL-1β biotin-conjugate (13-7016-81), IL-1β PE-conjugate (13-7016-81), IL-1β protein standard (39-8018-65), TNF-α antibody functional grade purified (16-7348-85), TNF-α PE-conjugate (12-7349-81), TNF-α protein standard (39-8329-65). Anti-human PSA and TNF-α antibodies (10-P20E and 16-7348-85, respectively) were biotinylated using the ChromaLink One-Shot Antibody Biotinylation kit (Solulink). Finally, the 10-P20D PSA antibody was conjugated with phycoerythrin using the R-PE Antibody All-in-One Conjugation kit (Solulink). ELISA diluent solution (00-4202-56, eBioscience) was used to re-suspend protein standards and dilute samples.

ELISA

Human PSA-total ELISA kit (ELH-PSATOTAL-001) was purchased from RayBiotech, Inc. The 96-well ELISA plate assay was performed according to the manufacturer instructions. Serum samples were diluted 2- and 10-fold; PSA protein standards were prepared using both the ELISA kit and the native human PSA protein. 100 μL volume samples were pipetted into the wells, incubated for 2.5 hours at room temperature, washed extensively, and incubated with biotinylated anti-PSA antibody for 1 hour, followed by another washing, incubation for 45 min with streptavidin, washing, and incubation with TMB substrate for 30 min. Finally, 50 μL of stop solution was added to each well to stop the reaction. The absorbance of each well was quantitated with a microplate reader (Synergy Mx, Biotek Instruments).

Human clinical specimens

Human serum samples were purchased from Asterand (UK). Our samples consisted of 10 patients who were diagnosed for prostate cancer and 10 control samples (5 female and 5 male). Medical records of each patient are included in ESI,† Table S1.

Spotting

Samples were spotted on the epoxy-coated glass slide using the same spotting protocol previously described.[7] Briefly, samples were spotted from a 384-well microtiter plate onto an epoxy-coated glass slide with a 4.9 nL delivery-volume spotting pin (946MP8XB, Arrayit, USA) using a microarray robot (QArray2, Genetix) at 60% humidity. The resulting spots were ~350 μm in diameter. The microfluidic device was aligned on top of the spotted glass slide and bonded overnight in the dark at 40 °C.

Control line priming

Control lines on the chip were primed with deionized water at 4 psi. Upon observation that control lines were fully primed, the pressure was increased to 23 psi. During the experiments, all flow lines were operated at 3.2 psi.

Optical read-out, quantification and statistics

The microfluidic device was scanned with an exposure time of 1 s using a fluorescent microarray scanner (Arrayworx, Applied Precision, USA) outfitted with a Cy3 filter (540/25 X, 595/50 M). The resulting TIFF-images were manually analyzed using a microarray image analysis software (GenePix Pro v6.0, Molecular Devices) and Matlab (Mathworks). Statistical and nonlinear regression analysis was performed using Prism v5.0 (Graphpad).

Results and discussion

Microfluidic design and operation

The microfluidic device consists of a flow and control layer fabricated by multi-layer soft-lithography to facilitate control and automation of the assays. The PDMS device is 68 mm long, 20 mm wide, and ~4 mm thick (Fig. 2.a, ESI,† File S1), and is bonded to a 25 mm × 75 mm glass slide. The device contains 1024 assay units separated from each other with a "sandwich" valve. Each assay unit comprises a spotting chamber and an assay chamber (white dotted circles in Fig. 2.b). The spotting chamber is aligned on top of the spotted sample. A valve separates the spotting chamber from the assay chamber. The assay chamber contains four deflectable button membranes (MITOMI)[7,9,10] that perform a total of 4096 assays per chip. The device contains a total of 7198 valves, which are operated using 14 pneumatic control lines. Reagents can be loaded onto the chip through nine fluidic ports, which are controlled by a multiplexer. Two outlets, one used for bubble purging and one for waste, are controlled with their respective valve.

MITOMI button-membranes facilitate immobilization of the different antibodies as well as incubation and washing steps without loss of bound material.[9] Spotted samples are dried before aligning and are kept in that state until the start of the experiment (ESI,† Fig. S1). Baking the device overnight at 40 °C is sufficient to bond the PDMS device to the epoxy glass slide. This bond is strong enough to withstand the fluidic pressures required during normal chip operations. After the control lines are actuated, the hygroscopic sample spots begin to slowly rehydrate due to water diffusion through the PDMS from the neck valve on the control (top) layer to the flow (bottom) layer. Two fluidic capacitors are located on top of the spotting chamber (in front to the neck valve) to relieve some of the pressure. Previous designs that did not include the capacitors resulted in leakage of the spotted samples into the assay chamber during the assay due to fast rehydration and high internal pressures. The relief valve, which leads to an overflow channel, is opened at the end of the incubation step to relieve built-up pressure and allow closing of the neck valves.

At the beginning of the assay, the control lines are primed at low pressures (4 psi) to avoid fast rehydration of the samples that could pervade into the assay chamber and lead to contamination. After the lines are primed (~3 min), the pressure is increased to 23 psi, and the neck valves and relief valves are closed to isolate the chambers with the spotted samples for the duration of the surface patterning steps.

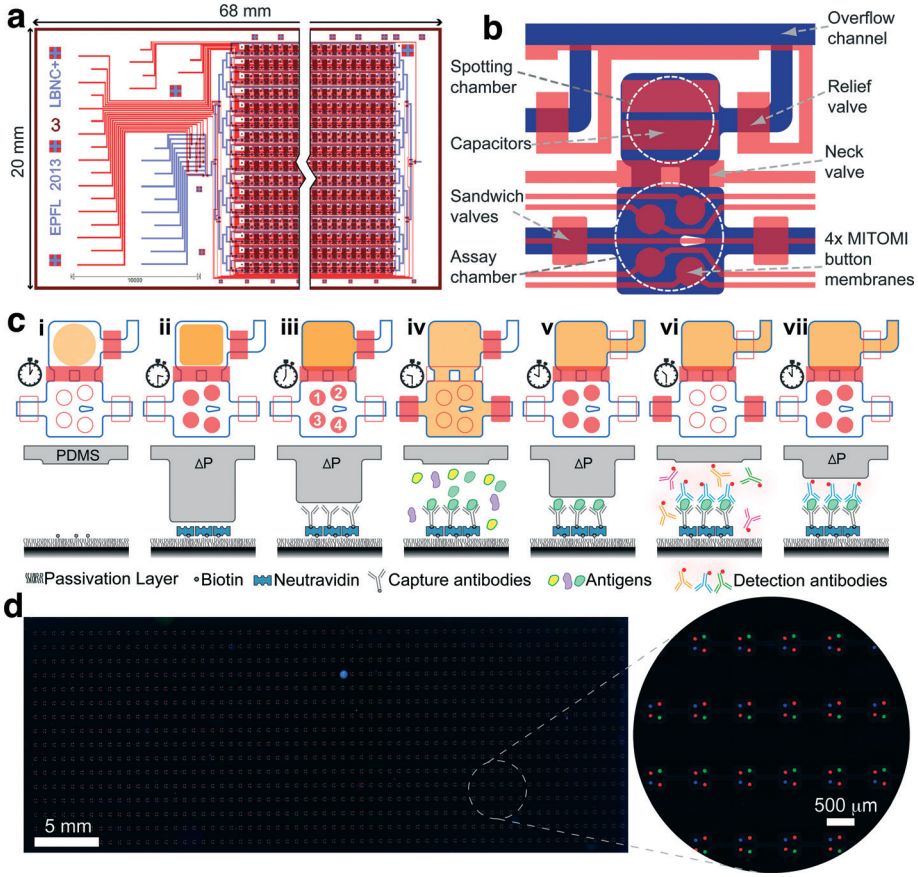

Fig. 2 Chip design. (a) Dimensions of the microfluidic device. Blue and red colors denote control and flow layers, respectively. (b) The assay unit can be divided into a spotting chamber and an assay chamber (highlighted by white dotted circles). MITOMI button membranes are located in the assay chamber. See text for a detailed description. (c) Assay workflow showing a simplified schematic of a single assay unit with the spotted sample (top row) and a cross-sectional view of the volume between one button membrane (PDMS) and the surface (bottom row). Biotinylated BSA is immobilized on the surface directly underneath the buttons (i). Spotted sample begin to rehydrate. Neutravidin molecules are bound to the biotin groups of the BSA (ii). Biotinylated capture antibodies are bound to neutravidin (iii). After incubation with the sample, (iv) the button membranes are actuated (v) to protect the bound analytes during the wash step. A cocktail of fluorescent detection antibodies is incubated with the antigen–antibody complex (vi). The button membrane is actuated again to protect the sandwich complex during the final washing step (vii). The clock shows approximate duration of every step in hours. (d) Fluorescent scanning image of the full chip with different colored neutravidin molecules immobilized under the button membranes. The image shows a total of 4096 assays. Alexa 488, Cy3, and Cy5 fluorescence channels were colored blue, green, and red, respectively.

Every single step described next is followed by a washing step for 10 min with PBS/Tween 0.05%. First, biotinylated BSA (2 mg mL^{-1}) is flowed through the chip for 40 min followed by neutravidin for 40 min (Fig. 2.c.i). Next, the four button membranes are actuated and biotin–BSA flowed again for 40 min. A layer of neutravidin remains under the area protected by the deflected button membranes (Fig. 2.c.ii). The primary antibody immobilization step uses biotinylated antibodies. Each antibody is flowed for 40 min at a concentration of 2 μg mL^{-1} (diluted in casein) with the corresponding button membrane open while the other 3 buttons remain closed (Fig. 2.c.iii). At this point, all samples throughout the chip have rehydrated. The sandwich valves are closed to prevent cross-contamination between chambers and the neck valve is opened to allow the sample to diffuse into the assay chamber (Fig. 2.c.iv). We incubate the sample for two hours (see next section) to ensure complete equilibration of the sample and the four analytes.

To remove any unbound material in the assay chambers, the MITOMI buttons are closed and the relief valves are opened for a few seconds. Thus, the internal pressure which continues to increase during the incubation step is released, in turn allowing the button membranes to fully deflect and trap the primary antibody–analyte complex (Fig. 2.c.v). Next, the neck valves are closed and the sandwich valves are opened. Washing for 30 min ensures removal of any unbound material. A cocktail of four fluorescent detection antibodies (each at a concentration of 400 ng mL^{-1}) is flowed through the chip for 20 min with the button membranes closed. The flow is stopped, the sandwich valves are closed, and the button membranes are opened for 20 minutes in order to let the detection antibodies bind to the primary antibody–analyte complex (Fig. 2.c.vi). Closing the button membranes protects the sandwich immunocomplex. Next, the sandwich valves are opened, and the assay chambers are washed for 30 min to remove any unbound material

(Fig. 2.c.vii). Fig. 2.d shows an example of a fluorescent image of the chip with the area under the button membranes patterned with different fluorescently labeled neutravidin molecules.

Incubation time

We used GFP (MW = 32.7 KDa) to determine the optimal time for the incubation step. GFP was spotted at concentrations ranging from 163 ng mL^{-1} to 327 pg mL^{-1} (5 nM to 10 pM), equivalent to a range of 3.9×10^6 to 7800 molecules. A biotinylated anti-GFP antibody was immobilized on one of the button membranes of the bottom row with the longest diffusion distance. We acquired time-lapse fluorescence measurements of the chip every 10 minutes for 150 min. ESI,† Fig. S2.a shows the response curves for the different concentrations. While binding for analyte concentrations above 1 nM occurs in a matter of minutes, it takes about 1 hour to capture ~90% of the molecules present at 10 pM. Thus, incubation of at least one hour is needed to detect concentrations as low as 10 pM. After 150 min of incubation, the button membrane was closed, and the assay chambers were washed for 30 min, showing that even after a thorough washing the button membranes are effective in trapping the bound antibody–antigen complex, even at the lowest detected concentration of 10 pM (ESI,† Fig. S2.b).

Calibration curves and ELISA comparison

We evaluated the performance of our chip by comparing our chip based measurements of four different biomarkers to values obtained with commercial ELISA kits. We found limits of detection (LOD, intensity of lowest analyte concentration that has a value higher than the mean of a negative control plus two standard deviations) to be 62.5 pg mL^{-1} (3.67 pM) for TNF-α, 15.6 pg mL^{-1} (742 fM) for IL-6, 15.6 pg mL^{-1} (897 fM) for IL-1β, and 31.25 pg mL^{-1} (1.04 pM) for PSA (Fig. 3). The sensitivity of our technology is therefore ~1 pM, or ~800 molecules per unit chamber. These LOD values are similar to those reported in the literature employing microfluidic devices;[6,11–13] however, our device requires only ~5 nL of sample, which is at least 1000 times smaller than what most microfluidic devices currently require.

Standard curves for the cytokines are comparable to ELISAs that use the same antibody pairs (see for example datasheets of ELISA kits for human TNF-α, IL-1β, IL-6: BM223INST, BMS224INST, BMS213INST, respectively, from eBioscience). Concentrations lower than 1 ng mL^{-1} for these cytokines and PSA showed no cross-reactivity with the other analytes.

Because the PSA standard used in the chip (native purified protein) was different from the ELISA kit (recombinant protein), we decided to compare both proteins as measured by ELISA. We found that both proteins have the same LOD of 125 pg mL^{-1} (4.16 pM) and similar standard curves (ESI,† Fig. S3). Interestingly, the ELISA measured sensitivity is ~15-fold higher than the sensitivity reported by the manufacturer (8 pg mL^{-1} or 266.7 fM). In contrast, the LOD measured on-chip was 31.25 pg ml^{-1} (1.04 pM), 5-fold higher than the reported ELISA LOD.

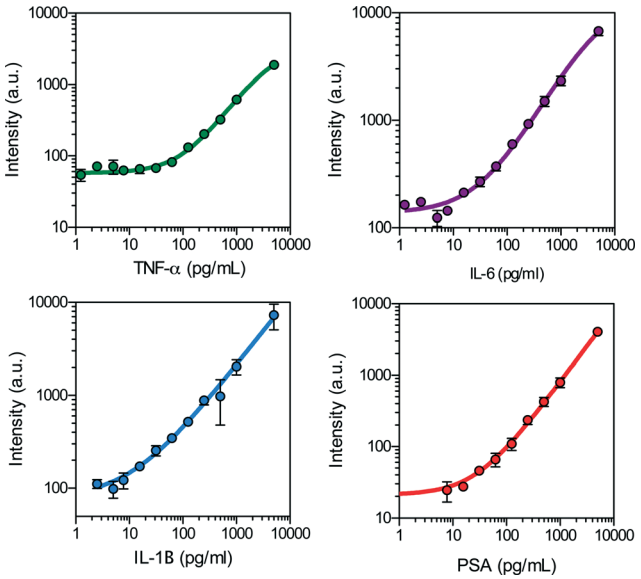

Fig. 3 Protein standards. Fluorescent intensities of the dilution curves for TNF-α, IL-6, IL-1β, and PSA measured with our chip. Error bars: 1 standard deviation (s.d.), $n = 5$.

Clinical results

To evaluate the utility of our technology, we measured the same 4 biomarkers in 20 human clinical samples using our chip and compared them to a standard ELISA (performed in our lab) and to values provided by the serum supplier. Ten of the clinical samples were from male patients diagnosed with prostate cancer, with total-PSA values measured at the time of sample collection (Fig. 4.a, top row). The other ten clinical samples were controls coming from five female and five male donors younger than 40 years of age (Fig. 4.a, bottom row), for which there were no total-PSA measurements available.

The serum samples were thawed and diluted 2- and 10-fold in standard ELISA buffer. The original serum sample and the dilutions, together with the four protein standard calibration samples, were spotted on an epoxy-coated glass slide, aligned to the chip, baked overnight, and run the next day. All samples were assayed in quintuplicates, for a total of 475 spotted samples and 1900 assays per chip. Fluorescence intensity units from the protein dilutions were analyzed with a 4-parametric logistic regression. Picogram per milliter values were derived from the curve fit.

Values measured on-chip and with ELISA are generally lower than the ones reported by the serum supplier (Fig. 4.b), possibly due to sample degradation or sub-optimal storage conditions since the original measurement. Others have also observed a slight decrease in total PSA values over time.[14] Most of the samples used in this study were collected in 2011 and some as early as 2006. However, there is a good

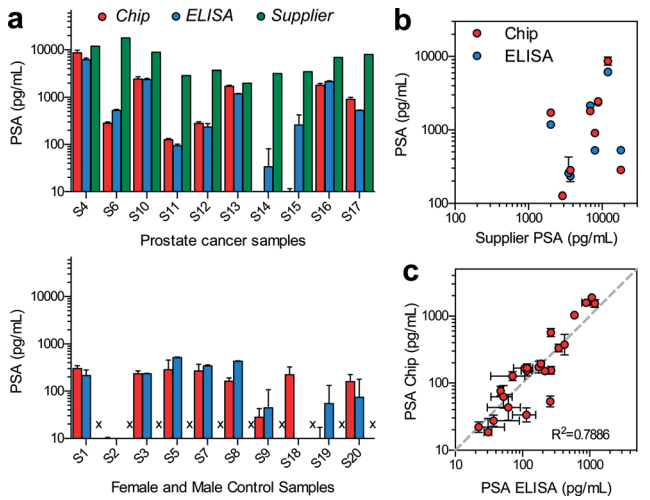

Fig. 4 Performance comparison on patient sera. (a) Grouped bar graph of total-PSA values measured with the chip, a conventional ELISA, and values provided by the supplier. Top and bottom rows correspond to data from 10 prostate cancer patients and 10 control samples, respectively. x denotes no information provided by the supplier. (b) The same data from the top row in (a) is shown in the form of a scatter plot. (c) Correlation between ELISA performed in our lab and the chip. Error bars: 1 s.d. (n = 5, chip and n = 2, ELISA).

correlation (R^2 = 0.79) between the values obtained with the chip and the ELISA performed in our lab (Fig. 4.c). Even for samples that were diluted 2- or 10-fold, our chip shows the same sensitivity as a conventional ELISA (ESI,† Fig. S4). Measurements for the other biomarkers are shown in ESI,† Fig. S5. The average coefficient of variation (CV) for the chip and ELISA is 23.45% and 29.79%, respectively. These results validate the utility of our technology to assay clinical human serum samples in high throughput.

Measurements for the other biomarkers are shown in Fig. 5. The current cut-off value of total-PSA used for diagnosing prostate cancer is 3–4 ng mL^{-1},[15] which is ~100 times higher than the LOD of our chip (31.25 pg mL^{-1}). Interestingly, some of the female control samples showed elevated values of PSA, >100 pg mL^{-1}. PSA has emerged as a potential biomarker for diagnosing breast cancer,[16] with a median of 1.3 ng mL^{-1} total-PSA for breast cancer patients[17] and of 670 pg mL^{-1} for women with breast cysts.[18] The sensitivity of our chip is thus well suited to detect both types of conditions. Levels of IL-6 were also generally higher for prostate cancer patients than for the controls. IL-6 level has been shown to correlate with the extent of disease in prostate cancer patients.[19] Female sample controls showed a correlation of IL-1β and PSA levels. IL-1β levels were in general higher for prostate cancer patients with a Gleason score ≥7, in agreement with recent findings.[20] TNF-α was not detected in any of the samples.

Benchmark of ELISA *vs.* serum analyzer chip

We quantify the advantages of our serum analyzer chip by comparing the reagent volume consumption, time, and total cost of running a chip against a typical ELISA, the current gold standard for protein quantitation (Table 1, ESI,† Table S1).

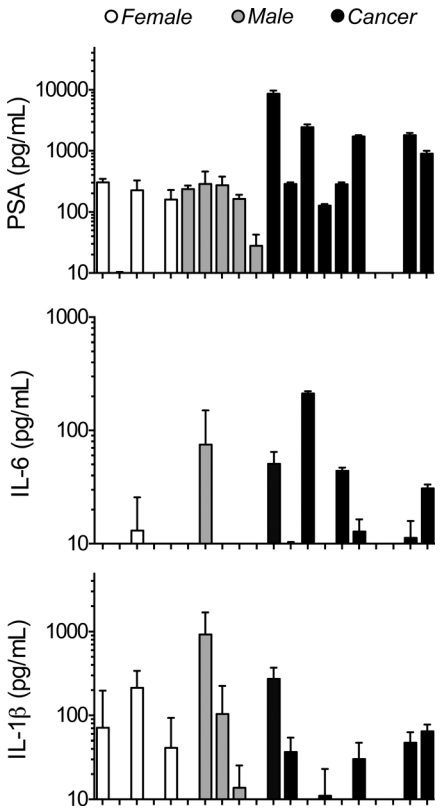

Fig. 5 Multiplexed biomarker measurements from human blood sera. Bar plot measurements of PSA, IL-6, and IL-1β for the 20 serum samples employing the chip. TNF-α was not detected in the samples. Data are arranged into three groups: female and male controls and prostate cancer patients. Error bars: 1 s.d., n = 5.

The reduction in sample volume is considerable with a 10 000-fold reduction, while achieving similar limits of detection as with current state-of-the-art microfluidic based approaches. This sample volume reduction, together with the design of our chip, also decrease the amount of capture and detection antibody required by over 4-orders of magnitude. Antibodies are the most expensive components in an immunoassay, and as recently reported by Wu *et al.*[21] there can be quality variations between batches of the same antibody. With 50 μg of antibody we can run almost 10 000 chips or ~10 000 000 assays.

Interestingly, over 80% of the total cost to run a chip currently stems from the surface passivation reagents (Biotin–BSA and Neutravidin, ESI,† Table S1), which suggests that further decrease in cost could be possible by other more affordable and simple surface passivation methods.[22–24] One key advantage of our chip is that it does not require an enzymatic amplification step to achieve high sensitivity, but rather uses fluorescently labeled detection antibodies (phycoerythrin), which helps reduce the cost and complexity of the assay.

Conclusions

We have demonstrated an integrated microfluidic platform capable of measuring 4 biomarkers in 1024 blood serum

Table 1 Comparison of reagent consumption, time, and cost using our chip and a 96-well plate conventional ELISA, per biomarker

	This platform (per assay unit)	ELISA (per well)	Fold improvement
Sample volume	5 nL	50 μL	10 000
Capture antibody amount	~5 pg	>50 ng	>10 000
Detection antibody amount	~100 fg	>5 ng	>50 000
Standard protein volume	5 nL	100 μL	20 000
Enzymatic amplification step	No	Yes	
Multiplexing	4	1	4
LOD (PSA, this work)	31.25 pg mL^{-1}	125 pg mL^{-1} (8 pg mL^{-1})[a]	Same
Time to run a single assay[b]	13 s	243 s	18
Automation	Microfluidics	None	—
Effective area per assay	0.48 mm^2	31.67 mm^2	66
Reagent consumption volume[c]	29 nL *per assay unit*	1550 μL *per well*	~53 500
Cost of reagents per assay	~US$0.0001	$3.82	>40 000
Total cost of reagents to run a chip or a 96-well plate ELISA[d]	~US$0.1	$489.00	

[a] As measured in our lab (sensitivity claimed by the manufacturer). [b] ESI, Table S2. [c] ESI, Table S3. [d] ESI, Table S1.

samples for a total of 4096 assays per chip. To the best of our knowledge, the throughput of our diagnostic microfluidic platform is ~100 times higher than current state-of-the-art microfluidic platforms.[11,13,25–35] To demonstrate the utility of our platform, we quantified different protein biomarkers from a few nanoliters of human serum and compared these to conventional ELISA, showing a good correlation and similar sensitivities as ELISA.

Scaling a standard immunoassay to nanoliter volumes has several significant consequences: i) thousands of assays can be performed in parallel on a single device, ii) reagent cost is reduced by several orders of magnitude, and iii) only a few nanoliters are required per sample. Additionally, our approach does not require sample preparation or sample pretreatment since serum samples can be directly arrayed and assayed.

It is now theoretically possible to test a single standard blood sample of 10 mL for a very large panel of biomarkers since 4 biomarkers can be tested for every 5 nL of sample, and the cost per biomarker is 0.0001 US$. For example, samples could be spotted on different glass slides, aligned to a microfluidic device, and each device measures a set of four different biomarkers. Additionally, small-volume serum samples of 50–100 μL would be easier to acquire, and to ship, and would be sufficient to run hundreds of tests using our serum analyzer platform. Indeed, small volume samples could be acquired by a simple pin-prick, and produce sufficient sample for microfluidic analysis, especially if diluted 2–10 fold in a stabilizing buffer.

It is also possible to perform several technical repeats for each sample at essentially no additional cost, which increases the precision of the measurement. Although we have exclusively used the sample mean and sample standard deviation to summarize our measurements in the manuscript, the standard error is more appropriate in some regards as it provides an estimate of the precision of the calculated sample mean. The mean and standard deviation describe the shape of the Gaussian distribution (centrality and spread). The standard error on the other hand provides an estimate of the precision of the measured sample mean. The standard error depends on n (SE = $\sigma/n^{1/2}$). Thus, the more measurements are taken for a given sample the smaller the SE and the precision of the measurement increases (the measured sample mean will be closer to the actual population mean and the confidence intervals will be narrower). By extension, the accuracy of the LOD can be expected to also slightly improve with increased n. The LOD is commonly defined as the sample mean of a negative blank plus 3 standard deviations. Increasing the number of measurements of the blank sample will improve the accuracy of the LOD value itself, as both the mean and standard deviation become more accurate. More importantly, if a sample is measured which has a population (true) mean equal to the LOD, and only a single measurement is taken then, assuming a symmetric measurement error, this measurement by definition has a 50% probability of being a false negative (to fall below the LOD). If many measurements are taken from the same sample, the precision of the sample mean increases. Thus, the sample mean is less likely to be significantly different from the actual population mean and thus is less likely to lead to a false negative (or conversely to a false positive, if the actual sample mean is below the LOD).

Extremely low sample volume requirements are particularly appealing for serum samples acquired during clinical trials or samples stored in biobanks. Our microfluidic nanoimmunoassay platform allows re-analysis of samples for additional biomarkers that have not been included in the initial study. Limited and non-renewable samples stored in biobanks can also now be analyzed many times, without risk of exhausting the sample stock. Equally attractive is the fact that samples can be pre-arrayed on glass slides, followed by long-term storage of the arrays, thus completely eliminating freeze–thaw cycles, which can lead to sample degradation.

In the future, our chip could be integrated with label-free biosensors to eliminate the need for secondary antibodies, further decreasing the cost of the platform and eliminating the need for optical readout.[36] Multiplexing of biomarkers could be increased at least 4-fold by generating concentric annuli by tuning the pressure of the button membrane

during surface patterning with each annulus measuring a different biomarker.[10] Improvements in sensitivity could be possible by adapting single-molecule detection techniques[37–40] or through the implementation of amplification schemes.

More generally, we have shown that our microfluidic MITOMI platform[9,41–43] is capable of measuring protein biomarkers in hundreds to thousands of samples with high-sensitivity and high dynamic-range.[7,10] The approach is matrix insensitive, meaning that sample origin is generally not important, and we have demonstrated that the platform is compatible with cell culture supernatants, mouse serum, mouse bronchoalveolar lavage (BAL), and now human serum. Our approach is thus high-throughput, precise, sensitive, cost-effective, and widely applicable, and thus should find many uses in diagnostics, as well as systems biology,[44] specifically in signal pathway analysis, where it is becoming increasingly necessary to quantitate many proteins in large numbers of samples.[45]

Acknowledgements

This work was funded by a grant from the Swiss National Science Foundation (CR23I2_140697).

References

1 V. Gubala, L. F. Harris, A. J. Ricco, M. X. Tan and D. E. Williams, *Anal. Chem.*, 2012, **84**, 487–515.
2 C. D. Chin, V. Linder and S. K. Sia, *Lab Chip*, 2012, **12**, 2118–2134.
3 R. Chen, G. I. Mias, J. Li-Pook-Than, L. H. Jiang, H. Y. K. Lam, R. Chen, E. Miriami, K. J. Karczewski, M. Hariharan, F. E. Dewey, Y. Cheng, M. J. Clark, H. Im, L. Habegger, S. Balasubramanian, M. O'Huallachain, J. T. Dudley, S. Hillenmeyer, R. Haraksingh, D. Sharon, G. Euskirchen, P. Lacroute, K. Bettinger, A. P. Boyle, M. Kasowski, F. Grubert, S. Seki, M. Garcia, M. Whirl-Carrillo, M. Gallardo, M. A. Blasco, P. L. Greenberg, P. Snyder, T. E. Klein, R. B. Altman, A. J. Butte, E. A. Ashley, M. Gerstein, K. C. Nadeau, H. Tang and M. Snyder, *Cell*, 2012, **148**, 1293–1307.
4 N. Blow, *Nat. Methods*, 2009, **6**, 173–177.
5 J. L. Garcia-Cordero and A. J. Ricco, in *Encyclopedia of Microfluidics and Nanofluidics*, ed. D. Li, Springer, US, 2008, pp. 962–969.
6 W. S. Liu, D. L. Chen, W. B. Du, K. P. Nichols and R. F. Ismagilov, *Anal. Chem.*, 2010, **82**, 3276–3282.
7 J. L. Garcia-Cordero, C. Nembrini, A. Stano, J. A. Hubbell and S. J. Maerkl, *Integr. Biol.*, 2013, **5**, 650–658.
8 Y. Nam, D. W. Branch and B. C. Wheeler, *Biosens. Bioelectron.*, 2006, **22**, 589–597.
9 S. J. Maerkl and S. R. Quake, *Science*, 2007, **315**, 233–237.
10 J. L. Garcia-Cordero and S. J. Maerkl, *Chem. Commun.*, 2013, **49**, 1264–1266.
11 R. Fan, O. Vermesh, A. Srivastava, B. K. H. Yen, L. D. Qin, H. Ahmad, G. A. Kwong, C. C. Liu, J. Gould, L. Hood and J. R. Heath, *Nat. Biotechnol.*, 2008, **26**, 1373–1378.
12 S. Cesaro-Tadic, G. Dernick, D. Juncker, G. Buurman, H. Kropshofer, B. Michel, C. Fattinger and E. Delamarche, *Lab Chip*, 2004, **4**, 563–569.
13 M. Hermann, T. Veres and M. Tabrizian, *Anal. Chem.*, 2008, **80**, 5160–5167.
14 D. Woodrum and L. York, *Urology*, 1998, **52**, 247–251.
15 J. R. Prensner, M. A. Rubin, J. T. Wei and A. M. Chinnaiyan, *Sci. Transl. Med.*, 2012, **4**, 127rv3.
16 Y. F. Chang, S. H. Hung, Y. J. Lee, R. C. Chen, L. C. Su, C. S. Lai and C. Chou, *Anal. Chem.*, 2011, **83**, 5324–5328.
17 M. H. Black, M. Giai, R. Ponzone, P. Sismondi, H. Yu and E. P. Diamandis, *Clin. Cancer Res.*, 2000, **6**, 467–473.
18 S. Radowicki, M. Kunicki and E. Bandurska-Stankiewicz, *Eur. J. Obstet. Gynecol. Reprod. Biol.*, 2008, **138**, 212–216.
19 V. Michalaki, M. Odontiadis, K. Syrigos, P. Charles and J. Waxman, *Br. J. Cancer*, 2004, **90**, 2312–2316.
20 Q. X. Liu, M. R. Russell, K. Shahriari, D. L. Jernigan, M. I. Lioni, F. U. Garcia and A. Fatatis, *Cancer Res.*, 2013, **73**, 3297–3305.
21 A. R. Wu, T. L. A. Kawahara, N. A. Rapicavoli, J. van Riggelen, E. H. Shroff, L. W. Xu, D. W. Felsher, H. Y. Chang and S. R. Quake, *Lab Chip*, 2012, **12**, 2190–2198.
22 J. Yakovleva, R. Davidsson, A. Lobanova, M. Bengtsson, S. Eremin, T. Laurell and J. Emneus, *Anal. Chem.*, 2002, **74**, 2994–3004.
23 R. P. Gandhiraman, C. Volcke, V. Gubala, C. Doyle, L. Basabe-Desmonts, C. Dotzler, M. F. Toney, M. Iacono, R. I. Nooney, S. Daniels, B. James and D. E. Williams, *J. Mater. Chem.*, 2010, **20**, 4116–4127.
24 C. C. O'mahony, V. Gubala, R. P. Gandhiraman, S. Daniels, J. S. Yuk, B. D. MacCraith and D. E. Williams, *J. Biomed. Mater. Res., Part A*, 2012, **100**, 230–235.
25 I. K. Dimov, L. Basabe-Desmonts, J. L. Garcia-Cordero, B. M. Ross, A. J. Ricco and L. P. Lee, *Lab Chip*, 2011, **11**, 845–850.
26 C. D. Chin, T. Laksanasopin, Y. K. Cheung, D. Steinmiller, V. Linder, H. Parsa, J. Wang, H. Moore, R. Rouse, G. Umviligihozo, E. Karita, L. Mwambarangwe, S. L. Braunstein, J. van de Wijgert, R. Sahabo, J. E. Justman, W. El-Sadr and S. K. Sia, *Nat. Med.*, 2011, **17**, 1015–1019.
27 Y. J. Song, Y. Q. Zhang, P. E. Bernard, J. M. Reuben, N. T. Ueno, R. B. Arlinghaus, Y. L. Zu and L. D. Qin, *Nat. Commun.*, 2012, **3**, 1283.
28 B. S. Lee, Y. U. Lee, H. S. Kim, T. H. Kim, J. Park, J. G. Lee, J. Kim, H. Kim, W. G. Lee and Y. K. Cho, *Lab Chip*, 2011, **11**, 70–78.
29 A. H. C. Ng, K. Choi, R. P. Luoma, J. M. Robinson and A. R. Wheeler, *Anal. Chem.*, 2012, **84**, 8805–8812.
30 L. Gervais and E. Delamarche, *Lab Chip*, 2009, **9**, 3330–3337.
31 B. S. Lee, J. N. Lee, J. M. Park, J. G. Lee, S. Kim, Y. K. Cho and C. Ko, *Lab Chip*, 2009, **9**, 1548–1555.
32 L. Lafleur, D. Stevens, K. McKenzie, S. Ramachandran, P. Spicar-Mihalic, M. Singhal, A. Arjyal, J. Osborn, P. Kauffman, P. Yager and B. Lutz, *Lab Chip*, 2012, **12**, 1119–1127.
33 E. M. Miller, A. H. C. Ng, U. Uddayasankar and A. R. Wheeler, *Anal. Bioanal. Chem.*, 2011, **399**, 337–345.

34 J. Ziegler, M. Zimmermann, P. Hunziker and E. Delamarche, *Anal. Chem.*, 2008, **80**, 1763–1769.
35 C. H. Zheng, J. W. Wang, Y. H. Pang, J. B. Wang, W. B. Li, Z. G. Ge and Y. Y. Huang, *Lab Chip*, 2012, **12**, 2487–2490.
36 F. Patolsky, G. F. Zheng and C. M. Lieber, *Anal. Chem.*, 2006, **78**, 4260–4269.
37 D. M. Rissin, C. W. Kan, T. G. Campbell, S. C. Howes, D. R. Fournier, L. Song, T. Piech, P. P. Patel, L. Chang, A. J. Rivnak, E. P. Ferrell, J. D. Randall, G. K. Provuncher, D. R. Walt and D. C. Duffy, *Nat. Biotechnol.*, 2010, **28**, 595–599.
38 S. H. Kim, S. Iwai, S. Araki, S. Sakakihara, R. Iino and H. Noji, *Lab Chip*, 2012, **12**, 4986–4991.
39 S. S. Acimovic, M. P. Kreuzer, M. U. Gonzalez and R. Quidant, *ACS Nano*, 2009, **3**, 1231–1237.
40 J. U. Shim, R. T. Ranasinghe, C. A. Smith, S. M. Ibrahim, F. Hollfelder, W. T. S. Huck, D. Klenerman and C. Abell, *ACS Nano*, 2013, **7**, 5955–5964.
41 M. Geertz, D. Shore and S. J. Maerkl, *Proc. Natl. Acad. Sci. U. S. A.*, 2012, **109**, 16540–16545.
42 S. J. Maerkl and S. R. Quake, *Proc. Natl. Acad. Sci. U. S. A.*, 2009, **106**, 18650–18655.
43 S. Rockel, M. Geertz, K. Hens, B. Deplancke and S. J. Maerkl, *Nucleic Acids Res.*, 2013, **41**, e52.
44 M. F. Ciaccio, J. P. Wagner, C. P. Chuu, D. A. Lauffenburger and R. B. Jones, *Nat. Methods*, 2010, **7**, 148–155.
45 M. J. Lee, A. S. Ye, A. K. Gardino, A. M. Heijink, P. K. Sorger, G. MacBeath and M. B. Yaffe, *Cell*, 2012, **149**, 780–794.